BIOCHEMISTRY
including biophysical chemistry & molecular biology

Article

pubs.acs.org/biochemistry

Detergents Stabilize the Conformation of Phosphodiesterase 6

Bo Y. Baker and Krzysztof Palczewski*

Department of Pharmacology, School of Medicine, Case Western Reserve University, Cleveland, Ohio 44106, United States

Supporting Information

ABSTRACT: Membrane-bound phosphodiesterase 6 (PDE6) plays an important role in visual signal transduction by regulating cGMP levels in rod photoreceptor cells. Our understanding of PDE6 catalysis and structure suffers from inadequate characterization of the α and β subunit catalytic core, interactions of the core with two intrinsically disordered, proteolysis-prone inhibitory PDEγ (Pγ) subunits, and binding of two types of isoprenyl-binding protein δ, called PrBP/δ, to the isoprenylated C-termini of the catalytic core. Structural studies of native PDE6 have been also been hampered by the lack of a heterologous expression system for the holoenzyme. In this work, we purified PDE6 in the presence of PrBP/δ and screened for additives and detergents that selectively suppress PDE6 basal activity while sparing that of the trypsin-activated enzyme. Some detergents removed PrBP/δ from the PDE complex, separating it from the holoenzyme after PDE6 purification. Additionally, selected detergents also significantly reduced the level of dissociation of PDE6 subunits, increasing their homogeneity and stabilizing the holoenzyme by substituting for its native membrane environment.

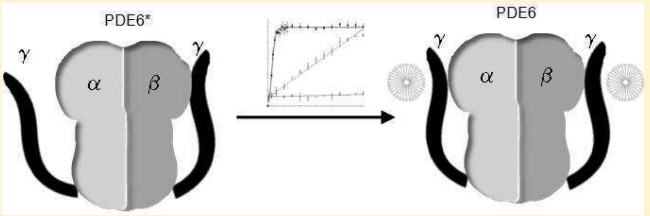

Phosphodiesterase 6 (PDE6) plays an important role in visual signal transduction by regulating cGMP levels in rod photoreceptor cells.[1] This protein belongs to the phosphodiesterase (PDE) superfamily that is comprised of 11 members that hydrolyze cAMP and cGMP and thus regulate cellular levels of these second messengers.[2] All PDEs possess a highly conserved C-terminal catalytic domain and various N-terminal domains that regulate enzyme activity. PDE6 is a structurally unique heterotetramer as compared with other PDE types, consisting of PDE6α (~99 kDa), PDE6β (~98 kDa), and two inhibitory PDE6 γ subunits (Pγ) (~10 kDa).[3−5] Although Pγ inhibits the catalytic domains of both PDE6α and PDE6β,[6−8] PDE$\alpha\beta\gamma_2$ still displays basal cGMP hydrolytic activity.[4−6,9]

Catalytic subunits PDE6α and PDE6β are posttranslationally farnesylated and geranylgeranylated, respectively, at their C-termini.[10] Presumably, these modifications anchor PDE6 to the membranes of rod outer segments (ROS).[3,10−12] PDE6 can be removed from ROS membranes by 17 kDa prenyl-binding protein δ (PrBP/δ) which, through binding to the isoprenylated carboxyl termini of the catalytic subunits,[13] has become a novel method for PDE6 isolation.[14] The resulting PDE6 complex then was highly purified, allowing it to be structurally studied by single-particle analysis.[14]

Significant structural information about PDEs is available. For example, a nearly full-length structure of PDE2[15] provided insights into the PDE topology and domain arrangement in addition to the regulation and function of this enzyme. The structures of several catalytic domains of the 11 PDE families have also been elucidated.[15−17] However, no high-resolution crystal structure is yet available for full-length holo-PDE6. The catalytic core of PDE6 is most structurally similar to that of PDE5 and to a lesser degree to those of PDE2, -4, -10, and -11.[2] The catalytic domain of a PDE5/6 chimeric protein complexed with the inhibitory Pγ peptide provided a structural basis for the Pγ regulatory mechanism.[18] The crystal structure of PrBP/δ in complex with Arl2-GTP showed that this protein has a fold similar to that of a modulator of rho family G proteins called RhoGDI[19] and protein UNC119,[20] both of which form a hydrophobic pocket for binding the geranylgeranyl moiety. Finally, the overall topology of PDE6 generated from single-particle analysis of negatively stained electron microscopy images at 30 Å[21] and 18 Å resolution[14] displayed domain arrangements similar to those seen in PDE2. The failure to functionally express PDE6 in various heterologous systems has impeded our understanding of the structural basis of PDE6 catalysis and regulation.[11,22,23] Moreover, PDE6α and PDE6β expressed in vitro did not form heterodimers as observed in vivo. Folding of this protein may require specific chaperone machinery that exists only in photoreceptor cells.[24]

Previous use of classical detergents used to facilitate protein extraction failed to improve PDE6 purification because this also solubilized rhodopsin and other membrane proteins present in ROS,[25] but an extensive list of reports in the literature also documents the effectiveness of including detergents in crystallization trials of soluble proteins, suggesting stabilization of a unique conformation of these proteins and possibly that the detergent also inhibits nonspecific interactions between protein monomers.[26−29] Here we characterized PDE6 purified in the presence of PrBP/δ and investigated the effects of different additives and/or detergents on the subunit integrity and catalytic activity of this enzyme.

Received: September 20, 2011
Revised: October 5, 2011
Published: October 6, 2011

EXPERIMENTAL PROCEDURES

Protein Preparation of Holo-PDE6. Holo-PDE6 was prepared from frozen bovine retinas (W. L. Lawson Co., Lincoln, NE) essentially as described previously.[14] First, bovine ROS membranes were isolated from 200 frozen retinas under dim red light as specified by Papermaster,[30] and then PDE6 was purified by the procedure reported by Goc et al.[14] Gel filtration chromatography of the crude protein was conducted on a Superdex 200 10/300 GL column (GE Healthcare) at a flow rate of 0.4 mL/min in gel filtration buffer containing 10 mM HEPES (pH 7.5) with 100 mM NaCl, 2 mM $MgCl_2$, and 1 mM DTT. Protein samples were concentrated to 10 mg/mL using a 30 kDa molecular weight cutoff (MWCO) filter (Millipore) and filtered through a 0.22 μM PVDF filter, and 250 μL was loaded onto the column. All SEC experiments were performed at 4 °C. Fractions containing PDE6 were pooled and concentrated to 10 mg/mL with a 30 kDa MWCO filter (Millipore). All purification steps were performed without detergent.

Protein Preparation of PDE6–PrBP/δ (PDE6/δ) and PDE6–PrBP/δ–GST (PG) Complexes. To free PG, ROS membranes were incubated with PrBP and δ-GST in a ratio of 10:1 (milligrams of total protein) for 60 min at room temperature, and the complex was extracted with 10 mL of isotonic buffer [20 mM HEPES, 5 mM $MgCl_2$, 1 mM DTT, and 100 mM NaCl (pH 7.5)]. The supernatant was separated from membranes by centrifugation at 15000 rpm and 4 °C for 20 min. This procedure was performed three times. The supernatants were combined and centrifuged at 15000 rpm for 60 min at 4 °C to remove the remaining ROS membrane particles, followed by overnight dialysis at 4 °C against 11.9 mM potassium phosphate, 137 mM NaCl, 2.7 mM KCl (pH 7.4), and 1 mM DTT. The resulting extract was applied to a 5 mL GSTrap column (GE) at a flow rate of 2.5 mL/min and washed with 10 column volumes of equilibrating buffer [11.9 mM potassium phosphate, 137 mM NaCl, and 2.7 mM KCl (pH 7.4)]. Bound proteins were eluted with 10 mL of 50 mM Tris-HCl (pH 8.0) containing 10 mM glutathione and 0.5 mM DTT. To obtain PG, fractions containing the PDE6–PrBP/δ–GST complex were pooled and further purified by gel filtration as described for the holoenzyme.

For the PDE6/δ preparation, fractions containing the PDE6–PrBP/δ–GST complex were pooled and treated with thrombin at room temperature overnight. Then the sample was concentrated from 30 mL to 500 μL by using a 30 kDa MWCO filter (Millipore) and further purified by gel filtration as described for the holoenzyme. For each run, concentrated protein (~2–5 mg/mL in 250 μL) was loaded onto the column. Fractions containing PDE6/δ were pooled and concentrated to 10 mg/mL. The resulting protein was homogeneous as assessed by sodium dodecyl sulfate–polyacrylamide gel electrophoresis (SDS–PAGE), native PAGE, and immunoblotting.[14] The protein concentration was determined spectrophotometrically at 280 nm and also by the Bradford method.[31]

Yields of PG, PDE6/δ, and PDE6 from 200 bovine retinas were ~1.5, ~1, and ~1.5 mg, respectively.

Trypsin-Treated PDE6 (PDE6$_t$). To prepare trypsin-treated PDE6 (PDE6$_t$) and holo-PDE6 were mixed with trypsin-agarose (Princeton Separations, Adelphia, NJ) at a ratio of 30 μg of protein to 1 μL of resin and incubated at room temperature for 30 min. Trypsin-agarose was removed when the mixture was passed through a 0.45 μM PVDF filter. PDE6$_t$ was further purified by using either buffer exchange with a 50000 Da MWCO filter (Millipore) or gel filtration to remove proteolytic Pγ fragments.[3] Briefly, the protein was concentrated to 100 μL (~2–5 mg/mL) with a 50 kDa MWCO Amicon Ultra filter and diluted with size exclusion chromatography (SEC) buffer [20 mM HEPES, 100 mM NaCl, 2 mM $MgCl_2$, and 1 mM DTT (pH 7.5)] to 500 μL. This process was repeated six times. Proteolytic fragments with low molecular masses passed through the 50 kDa MWCO membrane, whereas the remaining PDE6 catalytic core of 200 kDa was retained in the supernatant. Alternatively, the trypsin-treated protein was separated on a gel filtration column as described below; PDE6$_t$ eluted earlier and separated from smaller proteolytic fragments that eluted later.

For activity assays, PDE6$_t$ was prepared from holo-PDE6 in three different ways. First, PDE6 was mixed with trypsin at room temperature for a specified time period. Then soybean trypsin inhibitor was added to stop the reaction. Second, PDE6 was mixed with trypsin-agarose at room temperature for a specified time period, after which the trypsin-agarose was removed by membrane filtration. To remove proteolytic fragments, buffer was exchanged at least six times with a 50 kDa MWCO membrane (Millipore). Third, after removal of trypsin-agarose from PDE6$_t$ by membrane filtration, PDE6$_t$ was further purified by size exclusion chromatography. PDE6$_t$ eluted from the column as a single sharp peak at a position identical to that of untreated PDE6.

PDE6 Activity Assay. The pH-sensitive fluorescent dye SNAFL-1 (C-1270, Invitrogen) was used to monitor proton release caused by PDE6-catalyzed hydrolysis of cGMP and was measured fluorometrically[32] with a NovoSTAR (BMG Labtech) micro-plate spectrofluorometer reader. The assay was performed at 30 °C in assay buffer consisting of 20 mM MOPS (pH 8.0), 150 mM KC1, 10 mM $MgCl_2$, and 1 mM DDT. The protein (final concentration of 2 nM) was pre-incubated with assay buffer for 10 min, and the reaction was initiated by addition of cGMP (2 mM) and SNAFL-1 (20 μM) to achieve a final assay volume of 100 μL. The excitation wavelength was 480 nm, and emission was recorded at 540 nm with a gain value set to 1800. In the presence of PDE6, a steady increase in fluorescence intensity that reached a maximum in ~60 min was observed. The percentage of cGMP hydrolysis was plotted as the indicator of enzymatic activity versus time. For PDE6, the data were fitted by linear regression with the slope determined from the data. For PDE6$_t$, the data were fitted by nonlinear regression. The half-life ($T_{1/2}$) to reach a maximum fluorescence was calculated from the time-dependent curve by fitting the data to the Boltzmann sigmoid equation with Prism 3.0. Reported data are presented as the means and standard deviations from at least three independent experiments.

Detergent Concentrations. The concentration of PDE6 in the assays was ≤10 nM. To determine the tested concentrations for each detergent, detergent concentrations relative their critical micelle concentrations for PDE6 were initially calculated as follows: protein concentration (nanomolar) × aggregation number (typically 50–100) × 2 × 1.2–3.0 + CMC, where 2 accounts for the two catalytic subunits of PDE6 and 1.2–3.0 stands for the ratio of micelles to protein. For a detergent with a low CMC value, a 3-fold ratio was used, and for a detergent with a high CMC value, this ratio was 1.2. C_8E_4 is a typical high-CMC detergent with an aggregation number of ~82 and a CMC of ~8 mM. For this detergent, the calculated micellar concentration required for PDE6 (2 nM) is 2 nM × 82 × 2 × 1.5 or ~0.6 μM. Thus, at the concentration selected for testing (10 mM), C_8E_4 was sufficiently above its CMC to form micelles around PDE6. Anapoe X-100 is a typical low-CMC detergent (aggregation number of ~200, CMC of 0.3 mM).

dx.doi.org/10.1021/bi2014695 | Biochemistry 2011, 50, 9520–9531

For this detergent, the micellar concentration required for PDE6 is 2 nM × 200 × 2 × 3 or ~2.4 μM. At the tested concentration of 0.8 mM, Anapoe X-100 was also sufficiently above its CMC to form micelles around PDE6.

Measuring PDE6 Activity Directly by Product Formation. PDE6 degrades cyclic GMP to GMP and releases protons into solution. Accordingly, PDE6 activity was measured here by monitoring the proton release accompanying cGMP hydrolysis in a weakly buffered solution containing the pH-sensitive fluorescent dye SNARF-1. This method requires a certain amount of substrate to generate the pH changes that can be reflected by the dye. We tested $PDE6_t$ hydrolysis activity at various cGMP concentrations. For PDE6 activity measurements, the useful range of cGMP was approximately 1−10 mM. Below 1 mM, the resulting pH change was too small to generate a fluorescence signal much over background, and at concentrations above 10 mM, cGMP significantly reduced the fluorescence intensity of SNARF-1.

Thus, as an alternative, PDE6 activity was measured directly during hydrolysis of cGMP to GMP through isolation of both substrate and product by high-performance liquid chromatography (HPLC), essentially as described in ref 33 with modifications. Protein was first incubated in assay buffer [50 mM Tris (pH 7.5), 100 mM NaCl, 2 mM $MgCl_2$, and 1 mM DTT] for 15 min at room temperature. To initiate the reaction, cGMP was added to a final concentration 0.5 mM. The total volume for the assay was 100 μL. The reaction was performed at 37 °C and terminated at indicated time intervals by rapid protein denaturation at 95 °C for 5 min. Control experiments were performed without cGMP or enzyme added. In a typical assay, 2 nM $PDE6_t$ and 5 nM PDE6 were used for time course studies. To determine the apparent K_m value for cGMP, the activity of 0.4 nM $PDE6_t$ was measured at concentrations of cGMP ranging from 5 to 200 μM, and the resulting samples were further processed for nucleotide content.

cGMP and GMP were separated by a Zorbax ODS 5 μm, 4.6 mm × 250 mm reverse-phase HPLC column equilibrated with a 7.5% CH_3CN/H_2O solution containing 10 mM tetrabutylammonium bromide and a 100 mM K_2HPO_4/KH_2PO_4 mixture (pH 6.5). Nucleotides were eluted at a flow rate of 1.0 mL/min and identified by their UV spectra and elution positions relative to those of authentic standards. Reaction samples totaling 100 μL were centrifuged at 16100*g* for 10 min to remove denatured proteins. Supernatants were collected, and 30 μL of each sample supernatant was diluted five times with equilibrating buffer [100 mM K_2HPO_4/KH_2PO_4 (pH 6.5) containing 10 mM tetrabutylammonium bromide and 7.5% acetonitrile]. An aliquot of each supernatant (100 μL) was injected onto a Zorbax ODS 5 μm, 4.6 mm × 250 mm reverse-phase HPLC column (Agilent, Santa Clara, CA) and monitored at 254 nm. Nucleotides were eluted isocratically at a flow rate of 1.0 mL/min at room temperature.

Apparent K_m values were calculated from the concentration-dependent curve with Prism 3.0. Reported data are presented as the means and standard deviations (SD) from at least three independent experiments.

Electron Microscopy with Negative Staining. Purified PDE6 samples with or without detergents were adsorbed for 45 s onto glow-discharged carbon-coated copper grids (Quantifoil, Micro Tools, Ochtrup, Germany). Grids then were either washed with two 7 μL drops of water or directly stained with two drops of 1% uranyl formate. Electron micrographs were recorded with a T12 transmission electron microscope (FEI Tecnai) operated at 100 kV.

RESULTS

Isolation of Different Forms of PDE6. First, we tested whether the Pγ subunit could be removed through activation of membrane-bound PDE6 by first bleaching the ROS with light and then purifying the activated enzyme. However, Pγ was still detected in samples of the resulting purified active PDE6 by SDS−PAGE and immunoblots with an anti-Pγ antibody (data not shown).

Next, Pγ subunits were subjected to limited trypsin proteolysis to generate active $PDE6_t$. Digestion conditions were optimized by altering protein:trypsin weight ratios, incubation times and temperatures, and methods of tryptic treatment as described in Experimental Procedures. Under optimal conditions, the digestion yielded a stable product that was slightly smaller than untreated

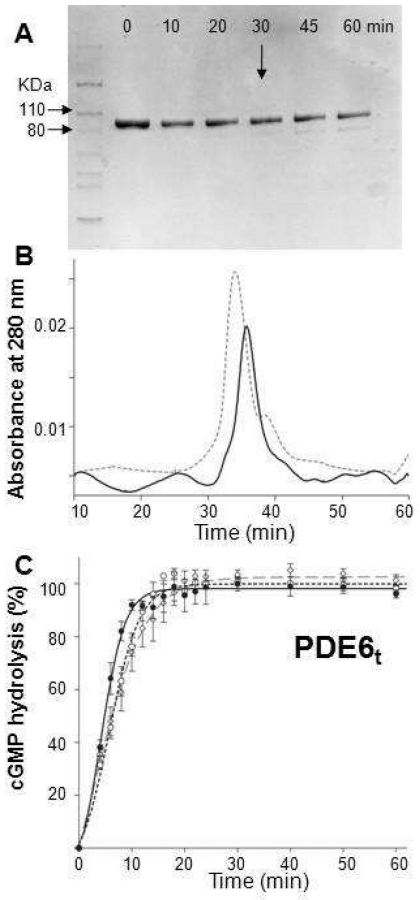

Figure 1. Preparation of trypsinized PDE6. (A) Time course of trypsin digestion monitored by SDS−PAGE. Purified PDE6 was mixed with trypsin at a 100:1 weight ratio and incubated at room temperature for 10, 20, 30, 45, and 60 min. Protein without trypsin was included as a control (lane 0). At 30 min (arrow), a weak band with a low molecular mass appeared. (B) Size exclusion chromatography profile of $PDE6_t$ (30 min, room temperature). $PDE6_t$ (—) eluted at nearly the same position as untreated PDE6 (---). (C) $PDE6_t$ activity with cGMP (2 mM) as a substrate. Enzyme activities monitored with the pH-sensitive fluorescent dye SNARF-1 were positively correlated with increasing fluorescence intensity over time. $PDE6_t$ was generated as follows. Purified PDE6 was first mixed with trypsin at a 100:1 weight ratio for 10 min. Soybean trypsin inhibitor was then added at a 1:10 mass ratio to stop the reaction (dashed line, ○). Alternatively, PDE6 was mixed with trypsin-agarose at a ratio of 30 μg of protein to 1 μL of agarose for 30 min, and the reaction was stopped when the sample was passed through a filter to remove the trypsin-agarose. Trypsinized peptides then were removed by either gel filtration (dashed line, ◇) or buffer exchange with a 50 kDa MWCO filter (Millipore) (solid line, ●). Activities for $PDE6_t$ prepared by all three methods were identical.

dx.doi.org/10.1021/bi2014695 | *Biochemistry* 2011, 50, 9520−9531

PDE6, as judged by SDS−PAGE (Figure 1A). Enzymatic activity was measured by using the SNARF-1 fluorescence assay. Although tryptic digestion produced fully activated PDE6, this treatment also led to protein heterogeneity because there are multiple trypsin digestion sites in the PDE6 catalytic core. Under controlled conditions, trypsin can effectively degrade the Pγ subunits,[8,34,35] but limited trypsin digestion also removes the C-termini from the PDE6 complex with a different cleavage ratio for PDE6α and PDE6β.[8] Thus, even though the SDS−PAGE and gel filtration profiles showed high apparent sample homogeneity after trypsin digestion, these procedures could not provide the resolution needed to reveal unique sites and heterogeneity resulting from such digestion. After longer digestion, a 70 kDa polypeptide fragment(s) appeared (Figure 1A). Gel filtration analysis showed that this 70 kDa fragment(s) could still form a higher-molecular mass complex (Figure 1B), probably by combining with truncated PDEαβ subunits.

Activity Measurements of Purified PDE6 with SNARF-1. PDE6 degrades cyclic GMP to GMP, releasing a proton into the bulk solution (Figure 2A). Accordingly, PDE6 activity was measured by monitoring the proton release accompanying cGMP hydrolysis in a weakly buffered solution containing the pH-sensitive fluorescent dye SNARF-1.[32] The pH-dependent fluorescence intensity profile of SNARF-1 is shown in Figure 2B. This assay allowed rapid screening for effects of many additives on PDE6 activity (Figure 2C).

$PDE6_t$ rapidly hydrolyzed cGMP with the fluorescence intensity reaching a maximum in approximately 5 min with a $T_{1/2}$ of ∼2 min (Figure 2C, dark line, ●). The change in pH during the assay was ∼0.1 pH unit for the whole time course. Initial rates for holo-PDE were not affected by an increased substrate concentration, implying that the assay operated at V_{max}. Indeed, the initial rate of cGMP hydrolysis also was proportional to the amount of enzyme added. In contrast, purified PDE6 displayed basal cGMP hydrolytic activity as demonstrated by slower hydrolysis of cGMP with a $T_{1/2}$ of 30 min (Figure 2C, dashed line, ○). This result indicates that the initial rate of PDE6 activity was ∼7% of that of $PDE6_t$ and was not completely suppressed by the inhibitory Pγ subunit under these assay conditions.

In control experiments, 5 mM EDTA nearly abolished $PDE6_t$ activity, probably by chelating Mg^{2+} or other metal ions and preventing them from interacting with $PDE6_t$ catalytic sites (Figure 3), whereas Ca^{2+} ions just reduced PDE6 activity (Figure 3A). Chaotropic additives were not effective in removing Pγ from the PDE6 complex. Urea at a concentration of 2 M had no effect on the enzymatic activity of $PDE6_t$, and arginine had only a minor effect (Figure 3A).

Effects of Detergents on PDE6 Stabilization. Because Pγ subunits could not be quantitatively removed, we then tried to identify conditions whereby these subunits could be retained with the catalytic core of PDE6. To explore the effects of detergents on purified PDE6 stability, we measured basal PDE6 activity in the presence of several representatives selected to cover a broad range of non-ionic, zwitterionic, ionic, and specialty detergents. $PDE6_t$ activity measurements served as controls for the effects of such additives on catalytic activity. One detergent from each class was chosen with a CMC in the range of 0.1−10 mM. Purified PDE6 was pre-incubated in assay buffer with the "test" detergent, and then cGMP and SNARF-1 were added to initiate the reaction. Fluorescence intensities were recorded over 60 min.

As shown in Figure 3B, the selected detergents had various effects on $PDE6_t$ activity. While CHAPS and OG reduced the

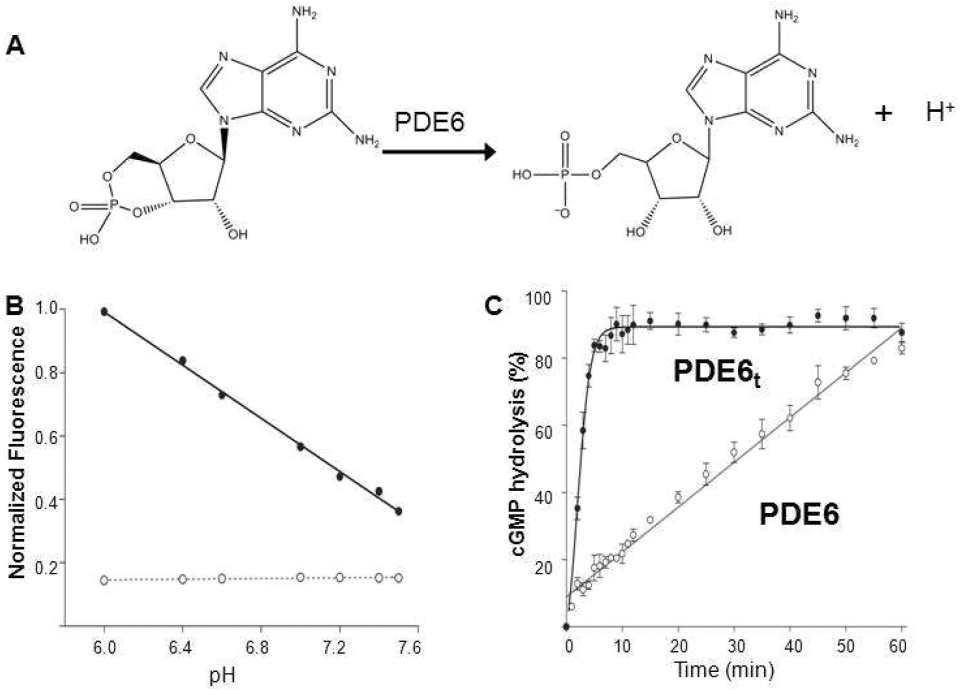

Figure 2. PDE6 activity measurements with the pH-sensitive fluorescent dye SNARF-1. (A) Diagram presenting PDE6-catalyzed hydrolysis of cyclic GMP to GMP with release of a proton. (B) PDE6 activity measurements with the pH-sensitive fluorescent dye SNARF-1 in 0.1 M HEPES over a pH range from 6.8 to 8.2. The fluorescence intensity of SNARF-1 decreased with an increase in pH (●), whereas the buffer used showed no fluorescence (○). (C) Enzyme activity measurements of PDE6 and $PDE6_t$ with SNARF-1. $PDE6_t$ achieved maximal cGMP hydrolysis in ∼5 min (●), whereas PDE6 exhibited much lower residual activity that resulted in total cGMP hydrolysis in ∼60 min (○). The percentage of cGMP hydrolysis is plotted as a function of time.

dx.doi.org/10.1021/bi2014695 | Biochemistry 2011, 50, 9520−9531

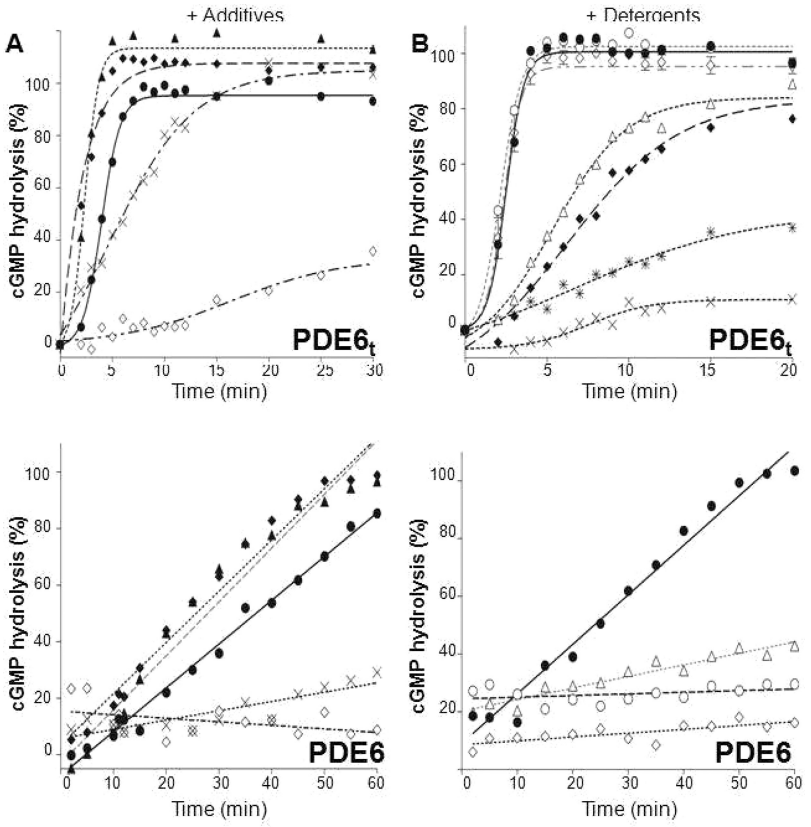

Figure 3. Effects of additives and detergents on $PDE6_t$ and PDE6 activity. (A) Effects of reagents on $PDE6_t$ and PDE6 activity. Activities of purified $PDE6_t$ (top) and PDE6 (bottom) were measured in the absence (solid lines) or presence (dashed lines) of designated reagents: urea (1 M, ▲), arginine (3 mM, ◆), $CaCl_2$ (0.1 M, ×), and EDTA (5 mM, ◇). The percentage of maximal $PDE6_t$ activity vs time is shown. (B) Effects of selected detergents on PDE6 activity. The activities of $PDE6_t$ (top) were measured in the absence (solid line) or presence of specified detergents (dashed lines): C_8E_4 (10 mM, ○), Anapoe X-100 (0.8 mM, ◇), CHAPS (25 mM, △), *n*-octyl β-D-glucopyranoside (20 mM, ◆), *n*-dodecyl-*N*,*N*-dimethylamine *N*-oxide (1 mM, ×), and dimethyldecylphosphine oxide (5 mM, ×). Those detergents that did not alter $PDE6_t$ activity were then tested for their ability to suppress PDE6 activity (bottom): PDE6 without detergent (solid line) and PDE6 with (dashed lines) *N*-undecyl β-D-maltopyranoside (1 mM, △), C_8E_4 (10 mM, ○), and Anapoe X-100 (0.8 mM, ◇). The percentage of cGMP hydrolyzed is plotted vs time.

rate of cGMP hydrolysis, others, including dimethyldecylphosphine oxide and *n*-dodecyl-*N*,*N*-dimethylamine *N*-oxide, abolished PDE6t activity altogether. Others such as Anapoe X-100 and C_8E_4 preserved $PDE6_t$ enzymatic activity. The $T_{1/2}$ for $PDE6_t$ to reach its maximal activity was determined for all detergents selected for testing (Table 1), and those with $T_{1/2}$ values close to $T_{1/2}$ values calculated in their absence were then subjected to further analysis for their effects on PDE6 activity. The rationale behind selection of the detergent concentrations used in these experiments is explained in Experimental Procedures.

Detergents found not to alter $PDE6_t$ activity but to reduce purified PDE6 activity are listed in Table 2. All such detergents were non-ionic. Anapoe X-100 and C_8E_4 significantly repressed PDE6 activity (Figure 3B, bottom), but other detergents only moderately repressed PDE6 activity, e.g., *n*-undecyl β-D-maltopyranoside. Polyoxyethylene glycols, such as Anapoe detergents, had the strongest effect on PDE6 basal activity suppression, whereas some maltosides and glucosides had an only moderate effect. For example, CYGLU-3, a non-ionic glucoside, failed to suppress PDE6 activity even at the high concentration of 30 mM, whereas Anapoe X-100 and Anapoe-35 at relatively low concentrations (0.3−0.8 mM) efficiently repressed PDE6 activity. At <1 mM, Anapoe X-100 reduced PDE6 activity ~12-fold and Anapoe-35 reduced it nearly 30-fold.

Stabilizing Effects of C_8E_4 on PDE6. As shown in Figure 4, the fluorescence intensity of purified PDE6 in the presence of C_8E_4 remained constant during the 60 min test period (Figure 4A, dashed line) but steadily increased in the absence

Table 1. $PDE6_t$ Activity in the Presence of Detergents[a] Measured by the SNARF-1 Assay

detergent	concn (mM)	$T_{1/2}$ (min)
none (control)	–	2.5 ± 0.1
Anapoe-35	0.3	1.1 ± 0.3
Anapoe X-100	0.8	2.3 ± 0.1
Cymal-6	2.0	3.0 ± 0.1
2,6-dimethyl-4-heptyl β-D-maltopyranoside	10	3.2 ± 0.2
MEGA-8	16	3.2 ± 1.0
PMAL-C8	0.1	2.5 ± 0.1
n-undecyl β-D-maltopyranoside	2	2.8 ± 0.8
n-dodecyl α-D-maltopyranoside	0.5	2.1 ± 0.2
n-undecyl β-D-thiomaltopyranoside	0.6	2.1 ± 0.4
C_8E_{12}	0.3	0.7 ± 0.3
C_8E_4	10	2.1 ± 0.2
sucrose monododecanoate	1	3.0 ± 0.3

[a]SNARF-1 fluorescence intensity was plotted vs time. The $T_{1/2}$ for reaching maximal fluorescence was determined by a nonlinear regression analysis. For detergents with no effect on $PDE6_t$ activity, $T_{1/2}$ values for $PDE6_t$ were similar in the presence and absence of detergent.

dx.doi.org/10.1021/bi2014695 | *Biochemistry* 2011, 50, 9520–9531

Table 2. Holo-PDE6 Activity Measured Using the SNARF-1 Assay in the Presence of Detergents[a]

detergent	concn	cGMP hydrolysis (%/min)
control (no detergent)	–	1.47 ± 0.05
Anapoe-35	0.3 mM	0.04 ± 0.01
Anapoe X-100	0.8 mM	0.15 ± 0.05
Cymal-6	2.0 mM	0.36 ± 0.05
2,6-dimethyl-4-heptyl β-D-maltopyranoside	10 mM	0.31 ± 0.03
MEGA-8	16 mM	0.36 ± 0.06
PMAL-C8	0.1 mM	0.33 ± 0.03
n-undecyl β-D-maltopyranoside	2 mM	0.43 ± 0.05
n-dodecyl α-D-maltopyranoside	0.5 mM	0.36 ± 0.05
n-undecyl β-D-thiomaltopyranoside	0.6 mM	0.16 ± 0.06
C_8E_{12}	0.3 mM	0.15 ± 0.05
C_8E_4	10 mM	0.04 ± 0.01
sucrose monododecanoate	1 mM	0.17 ± 0.06

[a]Holo-PDE6 activity in the presence of detergents was measured by the SNARF-1 assay (see Experimental Procedures). Some detergents significantly reduced PDE6 activity by ≥20-fold (i.e., C_8E_4 and Anapoe-35), and some exhibited a more moderate repression by a 5-fold reduction (i.e., DDM and MEGA-8). Data represent the means and SD of at least three separate experiments.

of this detergent. SNARF-1 also retained its sensitivity to pH changes in the presence of C_8E_4 (Figure 4B). When $PDE6_t$ was pre-incubated for 10 min in assay buffer containing C_8E_4 or purified PDE6 was digested by trypsin and the resultant $PDE6_t$ enzyme was added to the assay mixture containing C_8E_4, full activity was observed. This result could be ascribed to steric hindrance of Pγ by C_8E_4 micelles, preventing release of Pγ from the catalytic site of PDE6. Thus, the C_8E_4-induced suppression of PDE6 basal activity could be due to a stabilized interaction of Pγ with PDE6, with C_8E_4 forming a complex with PDE6 through an interaction with Pγ.

PrBP/δ Binding to PDE6. PrBP/δ can extract PDE6 from ROS membranes by binding to the isoprenylated carboxyl termini of the catalytic subunits,[13] but on the basis of EM observations, PrBP/δ failed to form a stable complex with PDE6 and the protein solution contained a mixed population of complexes with one or two PrBP/δ proteins bound. Instead, it was observed that PG (PDE6–PrBP/δ–GST) was more stable.[14]

The elution profiles of three forms of PDE6 in the absence of detergents are shown in Figure 5A. PDE6 and PDE6/δ eluted from the column as single sharp peaks, whereas a large fraction of PG formed a high-molecular mass aggregate. In the presence of the PrBP/δ–GST complex, PDE6 tended to aggregate, but these aggregates broke apart upon proteolytic removal of GST. On the basis of SEC analysis, the aggregation level of PG also increased with its protein concentration (data not shown). To reduce PG aggregation, various buffer conditions were tested. PG was buffer exchanged or dialyzed against the test media, and the resulting protein conformation was examined by SEC. Among the conditions tested, changes in pH (from 6.5 to 9.0) and NaCl concentration (from 0 to 0.5 M) did not affect the elution profile of PG; i.e., the protein remained as a mixture of the catalytic core dimer and aggregates. Addition of reagents and detergents had various effects. Glycerol allowed more aggregation, but glucose did not change the elution profile of PG. Whereas DDM, CHAPS, and Anapoe detergents partially reduced the level of PG aggregation, virtually no aggregation occurred in the presence of C_8E_4 (Figure 5C). Instead, the protein sample displayed a single sharp peak followed by a second peak with a lower molecular mass. SDS–PAGE analysis identified PDE6 in the first peak (peak 1) and the PrBP/δ–GST protein in the second peak (peak 2), indicating dissociation of the PrBP/δ–GST complex in the presence of C_8E_4. A similar phenomenon was observed with PDE6/δ. When this protein was incubated with C_8E_4, two peaks were observed upon SEC (Figure 5D), indicating that PrBP/δ had dissociated from the PDE6–PrBP/δ complex.

Because PrBP/δ did not form a tight complex with PDE6, it could be argued that dissociation of PrBP/δ from PDE6 was spontaneous rather than caused by the presence of C_8E_4. Thus, we determined if C_8E_4 could deplete the PrBP/δ–GST protein from the PG complex. PG was incubated with GST resin, and unbound proteins were removed by washing with buffer. PG without detergent was included as control to monitor binding of the PrBP/δ–GST complex to the resin. As shown in Figure 6A, no protein was detected after several washes. C_8E_4 (10 mM) was then added to the resin and left to incubate for 1 h. Then the resin was washed and subsequently eluted with

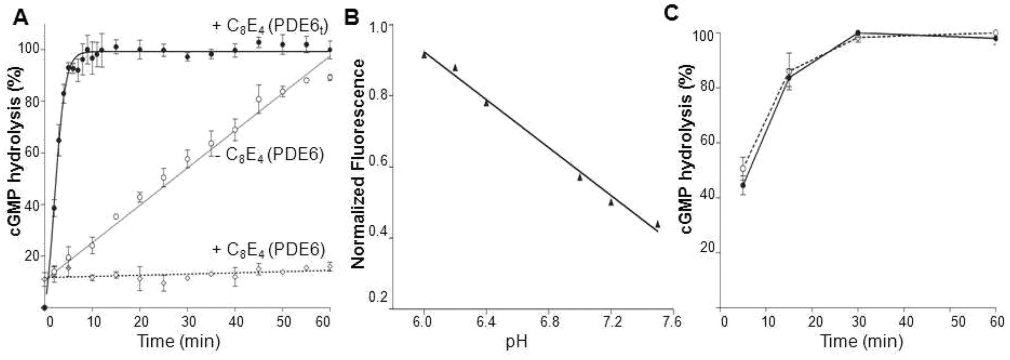

Figure 4. Effect of C_8E_4 on PDE6 activity. (A) Measurements of $PDE6_t$ (solid line, ●) and PDE6 (dashed line, ○) activity in the presence of C_8E_4. PDE6 activity without C_8E_4 is shown as a dotted line (○). In the presence of C_8E_4, $PDE6_t$ was fully functional whereas PDE6 activity was completely abolished. (B) In the presence of C_8E_4, the fluorescence intensity of SNARF-1decreased with an increase in pH, indicating that the dye responded appropriately to changes in pH. (C) $PDE6_t$ activity in the presence of C_8E_4. Protein was pre-incubated in assay buffer with C_8E_4 for 10 min before $PDE6_t$ activity was monitored (solid line). Alternatively, PDE6 was digested with trypsin in the presence of C_8E_4 before soybean trypsin inhibitor was added to stop the protease reaction and the resulting $PDE6_t$ was added to assay buffer along with C_8E_4 for activity measurements (dashed line). Both preparations of $PDE6_t$ were fully active.

dx.doi.org/10.1021/bi2014695 | *Biochemistry* 2011, 50, 9520–9531

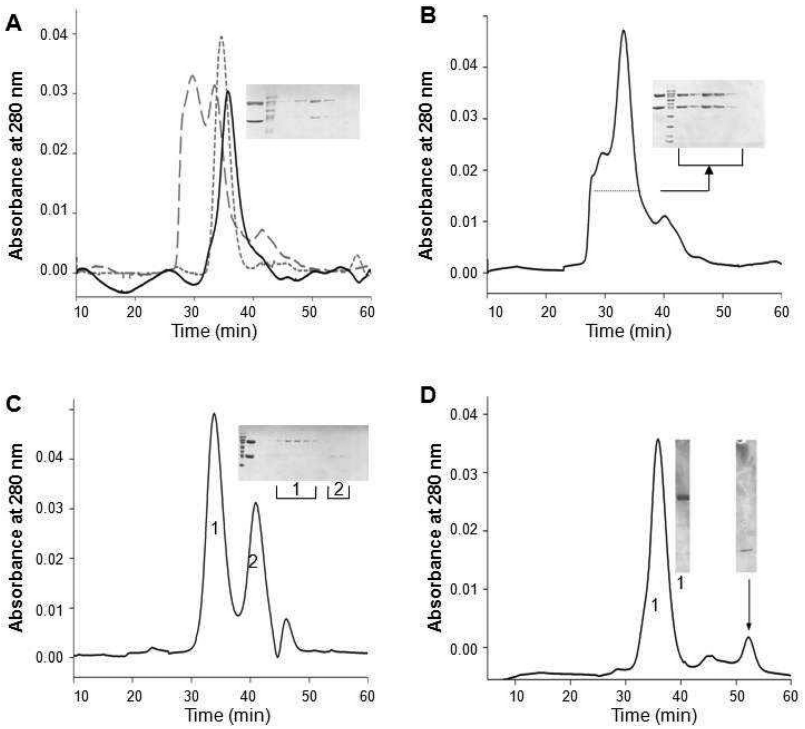

Figure 5. SEC analysis of effects of detergents on reducing the level of PG aggregation. (A) Elution profiles of three forms of PDE6 in the absence of detergent. PDE6 (---) and PDE6/δ (—) eluted as single peaks, whereas PG (–––) eluted as two major peaks indicating a mixture of a high-molecular mass aggregate and a monomer. The inset shows SDS–PAGE analysis of SEC fractions from the two PG peaks. The top band is PDE6 and the bottom band GST-δ. Some detergents, such as Anapoe-35 (B), reduced the level of aggregation of PG. The inset of panel B shows SDS–PAGE analysis of SEC fractions (indicated with a dotted line). In the presence of C_8E_4 (C), PG aggregation was almost completely abolished. PDE6 was found mainly in peak 1 (inset, labeled as 1). The second major peak eluting after the PDE6 peak represented the GST–PrBP/δ complex as indicated by SDS–PAGE analysis (inset, labeled as 2). (D) SEC analysis of the PDE6/δ conformation in the presence of C_8E_4. Fractions (0.5 mL) were collected. SDS–PAGE of fractions from the two major peaks is shown in the inset. The left band (labeled as 1) shows the fraction from the main peak with an estimated molecular mass of 200 kDa, whereas the right band illustrates the fraction from the last peak with an estimated molecular mass of 15 kDa (as indicated with an arrow). For all insets, analysis of the protein sample before SEC is shown next to the protein marker. The top band corresponded to PDE6 and the bottom band to GST-δ.

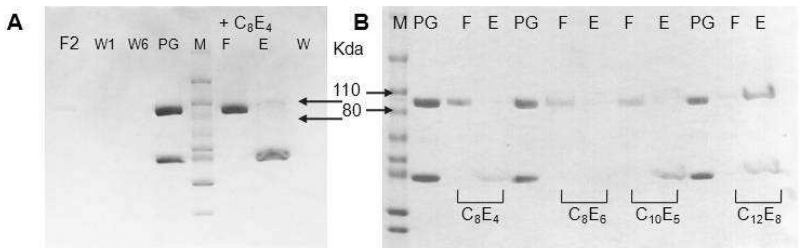

Figure 6. SDS–PAGE analysis of the detergent-depleted GST–PrBP/δ protein dissociated from the PG complex. (A) C_8E_4 removed the GST–PrBP/δ protein from the PG complex. PG was mixed with GST-FF resin, and unbound proteins were removed when the resin was washed with PBS. Then the resin was incubated with PBS and 10 mM C_8E_4 for 1 h at room temperature. The flow-through was collected (lane F, under C_8E_4), and the resin was washed again with PBS and C_8E_4. Elution was accomplished with reduced glutathione (10 mM): F, flow-through; W, wash fractions; E, elution fraction. (B) The extent of dissociation of the PG complex was decreased by incubation with C_nE_m detergents with longer alkyl chains: C_n, $CH_3(CH_2)_{n-1}$ alkyl chain; E_m, $(OCH_2CH_2)_mOH$ oligoethylene glycol. In the presence of C_8E_4 or C_8E_6, PDE6 was identified mainly in SEC flow-through fractions as shown by SDS–PAGE, but in the presence of $C_{12}E_8$, the PG complex remained intact in the elution fraction. Lanes F and E: flow-through and elution fractions, respectively, in the presence of C_nE_m.

reduced glutathione (10 mM); fractions were analyzed by SDS–PAGE. As shown in Figure 6A, PDE6 released from the resin was mainly found in the C_8E_4 flow-through whereas the PrBP/δ–GST protein was mainly present in the elution fraction. Thus, C_8E_4 dissociated the PrBP/δ–GST complex from PDE6 possibly by C_8E_4 micelles embedding the lipid moieties of PDE6.

We tested other polyoxyethylene detergents, including C_nE_m, to determine their effects on PG dissociation. For C_nE_m detergents, the length of the alkyl chain determines the detergent CMC and aggregation number, whereas the head-group has a strong influence upon interactions with proteins. As shown in Figure 6B, PDE6 in the presence of C_8E_4 and C_8E_6 was mainly present in the flow-through fractions, indicating its dissociation from the PrBP/δ–GST protein, but in the presence of $C_{10}E_5$, PDE6 was found in the flow-through fraction (strong) as well as in the elution fraction (weak). In the presence of $C_{12}E_8$, however, the PG complex remained intact

dx.doi.org/10.1021/bi2014695 | *Biochemistry* 2011, 50, 9520–9531

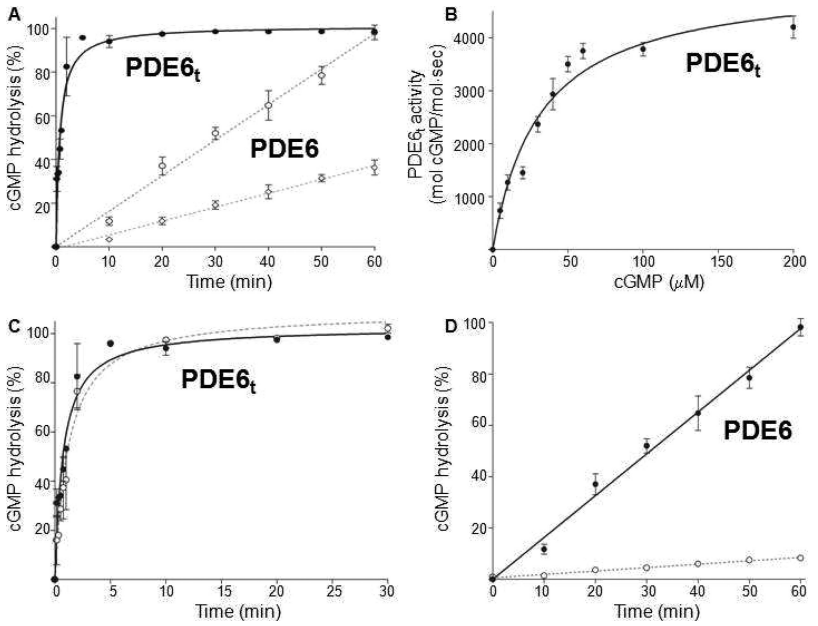

Figure 7. Catalytic properties of purified $PDE6_t$ and PDE6 assessed directly by product formation. (A) Percentages of cGMP hydrolysis by $PDE6_t$ and PDE6 plotted as a function of time: $PDE6_t$ (—) and PDE6 (---) [2 mM (◇) and 5 nM (○)]. (B) Rate of cGMP hydrolysis by $PDE6_t$ plotted as a function of cGMP concentration. The K_m value is 31 ± 4 μM, and the V_{max} value is 5122 ± 285 mol of cGMP mol^{-1} s^{-1}. (C) $PDE6_t$ activity in the presence and absence of C_8E_4. The percentage of cGMP hydrolysis by $PDE6_t$ is plotted as a function of time: $PDE6_t$ without C_8E_4 (—) and $PDE6_t$ with C_8E_4 (---). (D) cGMP hydrolysis in the presence and absence of C_8E_4. The percentage of cGMP hydrolysis by PDE6 is plotted as a function of time: PDE6 without C_8E_4 (—) and PDE6 with C_8E_4 (---).

and was found mainly in the elution fractions. Thus, detergents with longer chain lengths were identified that did not compete with the PrBP/δ–GST protein for binding to the lipidlike heads of PDE6 C-termini, probably because of their more hydrophobic hydrocarbon chain "tails". Alternatively, perhaps such detergents do not insert well into the prenyl-binding pocket of PrBP.

Verification of Suppression of PDE6 Basal Activity by the C_8E_4 Detergent in a Different Enzymatic Assay. The SNARF-1 assay is only useful for initial screening because it has a relatively low sensitivity and utilizes almost all the substrate during the course of the reaction. Therefore, the catalytic properties of PDE6 and $PDE6_t$ were also examined by direct HPLC analysis of cGMP hydrolysis (Figure 1 of the Supporting Information). Trypsin-activated $PDE6_t$ rapidly hydrolyzed cGMP, whereas PDE6 still displayed a certain level of activity. The catalytic parameters for $PDE6_t$ were determined (K_m = 31 ± 4 μM, and V_{max} = 5122 ± 285 mol of cGMP mol^{-1} s^{-1}), in agreement with previous studies.[18,36−40] In the presence of C_8E_4, $PDE6_t$ retained full activity (Figure 7C), rapidly hydrolyzing cGMP with the GMP level achieving a maximum in ∼1 min and a $T_{1/2}$ of ∼0.8 min without detergent. In the presence of C_8E_4, $PDE6_t$ rapidly hydrolyzed cGMP with a $T_{1/2}$ of ∼1.2 ± 0.2 min in the presence of C_8E_4.

PDE6 also displayed cGMP hydrolytic activity in an enzyme concentration-dependent manner. At 5 nM, it slowly hydrolyzed cGMP (Figure 7A), but in the presence of C_8E_4, this basal activity was markedly depressed (Figure 7D); the level of PDE6 hydrolysis was reduced approximately 10-fold from 1.4 to 0.13. Thus, both the SNARF-1 and direct product-based enzymatic assays showed that activated PDE6 remained fully functional in the C_8E_4 detergent and purified PDE6 itself retained its inhibitory subunits (Figure 2 of the Supporting Information). The activity of PDE6 was significantly suppressed in the presence of C_8E_4.

Electron Microscopy of PDE6 in Detergents. Taken together, the forgoing data have demonstrated that certain types of detergents tend to blunt the activity of PDE6, presumably by masking its isoprenylated C-termini and stabilizing the Pγ subunits. Thus, the resulting PDE6 should be more suitable for structural analysis.

Negative staining EM allows rapid screening of protein homogeneity with only small amounts of sample. Because PDE6/δ was highly purified, we studied its conformation in detergents by this procedure. In most detergents tested, such as C_8E_4 (Figure 8, left panel of bottom layer) and DDM (Figure 8, middle panel of top layer), PDE6/δ appeared as one major population of particles exhibiting an elongated shape with a wide top and a narrower end. The shapes of these particles were similar to those without detergent (Figure 8, top left panel) and identical to those seen in our previous EM study.[14] Samples with all tested detergents except CHAPS appeared fully homogeneous, indicating compatibility with PDE6/δ, but in CHAPS, most of the particles were smaller than those observed in DDM or C_8E_4 or without detergent. Many displayed a V-shaped structure (Figure 8, CHAPS right panel of bottom layer), indicating that CHAPS might have caused dissociation of the PDE6 complex, thereby providing a possible explanation for the reduced activity of $PDE6_t$ in its presence.

DISCUSSION

PDE6 is an important enzyme in phototransduction. However, structural information about full-length PDE6 is lacking. As a prelude to detailed structural studies, we first measured the enzymatic activity of our purified bovine ROS PDE6 preparation and observed a basal level of cGMP hydrolytic activity. While being firmly attached to PDEα and -β subunits, Pγ

dx.doi.org/10.1021/bi2014695 | Biochemistry 2011, 50, 9520−9531

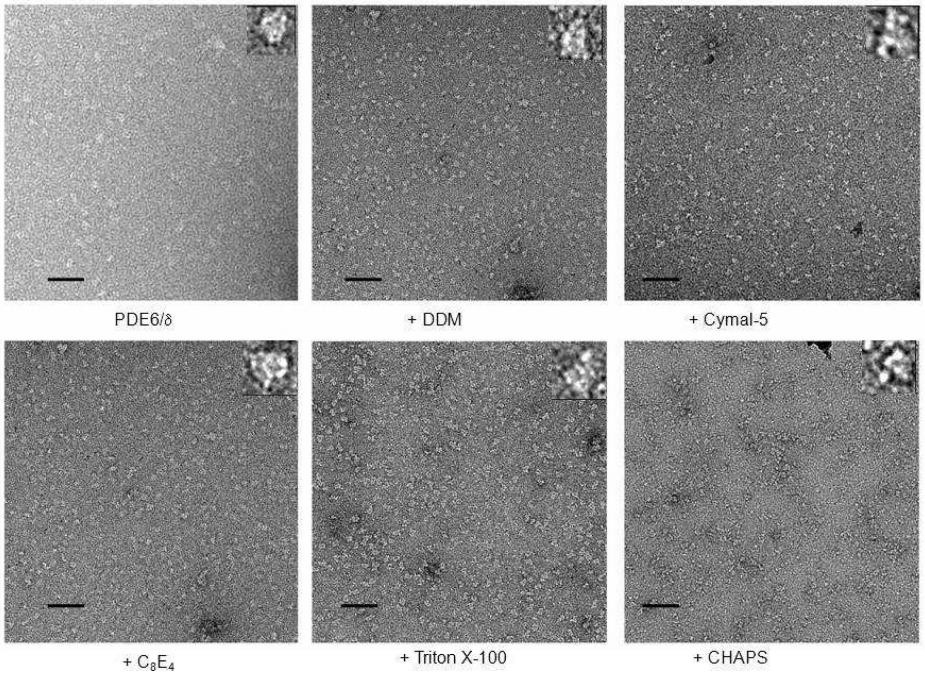

Figure 8. EM images of negatively stained PDE6/δ complexes in the absence and presence of the indicated detergents. The protein retained homogeneity in all detergents tested except CHAPS, in which the complex seems to have dissociated into smaller particles. The insets show higher-magnification images of single particles. Scale bars are 100 nm.

subunits only weakly block the catalytic activities of the PDEα and -β core. Gtα effectively displaces Pγ during the activation process, but this inhibitory subunit is not removed because a larger complex with other proteins involved in termination of the activation process is formed, including the G protein transducin.[41,42] Because this basal activity could be a "marker" for structural variability, we screened for additives or detergents that would completely suppress such activity while preserving the intrinsic activity of the PDE6 holoenzyme.

On the basis of our activity assays, the modest levels of basal activity exhibited by PDE6 purified from bovine ROS probably indicated that Pγ was not tightly bound to the catalytic sites of PDE6. The C-terminus of Pγ may only loosely associate with the catalytic site of PDE6, or perhaps only one Pγ is tightly bound, with the other loose or free, allowing this basal PDE6 activity. Meanwhile, the whole Pγ inhibitory unit could still be bound to PDE6 via a high-ionic affinity interaction with the central region of Pγ. Indeed, Pγ is known to inhibit PDE6 with the resulting Pγ–PDE6 interactions having been defined by many biochemical studies. The central region of Pγ (residues 24–45) is rich in Pro residues and positively charged amino acids and binds to the GAF-A domain of PDE6 with high affinity ($K_d \sim 50$ pmol).[32] The C-terminus of Pγ (residues 74–87) binds to the catalytic domain of PDE6 and blocks entry of the substrate into the catalytic site.[3,6,22,43–46] A nuclear magnetic resonance (NMR) study indicates that W70 plays a key role in this interaction.[9] Therefore, the protein may exhibit different dynamic conformations that result in sample heterogeneity. Pγ could have different association affinities for PDE6α and PDE6β. This dynamic conformation of Pγ along with its intrinsically disordered structure further complicates the possibility of crystallizing PDE6.

Here we have shown that certain types of detergents could help to stabilize PDE6. In the presence of C_8E_4, the basal activity of PDE6 was almost completely abolished, whereas $PDE6_t$ remained fully active. The fluorescence-based PDE6 activity measurements provided a quick and effective way to screen for detergents that stabilize PDE6. Fortunately, this method required only small amounts of protein, allowing rapid screening of samples with additives and detergents along with appropriate replicates and controls, but the same method requires high concentrations of substrate (cGMP) to generate pH changes sufficient for quantification by the SNARF-1 dye. Therefore, to determine catalytic parameters of PDE6 in the presence of detergents such as C_8E_4, we used the more rigorous methodology directly measuring the hydrolysis product, GMP, by HPLC. In agreement with results of the SNARF-1 assay, the presence of C_8E_4 did not alter $PDE6_t$ activity, and the basal activity of PDE6 was greatly suppressed.

It is still unclear why some detergents repress PDE6 activity whereas others do not. Pγ certainly plays an inhibitory role in the PDE6 structure. The amino acid sequence of Pγ may explain its preference for interaction with polyoxyethylene glycols such as C_8E_4 and Anapoe X-100. On the basis of our enzymatic activity assay results, only non-ionic detergents stabilized PDE6; zwitterionic and ionic detergents decreased or abolished $PDE6_t$ activity, indicating a major conformational change or denaturation. Among the non-ionic detergents tested, polyoxyethylene detergents had the greatest stabilizing effect on the interaction with Pγ.

The isoprenylated carboxyl termini of PDE6$\alpha\beta$ pose one of the major challenges in structural characterization of the enzyme purified from ROS. In the absence of membranes, hydrophobic isoprenyl groups are excluded from the aqueous phase and likely form a myriad of conformations when their tails are wedged nonspecifically into the protein core. The conformational heterogeneity of the protease-prone Pγ subunit and its possible heterogeneous truncation represent two of several major challenges for PDE6 subunit integrity. Amino acid analyses and biochemical studies of Pγ indicated that it is an intrinsically disordered protein (IDP),[46,47] whereas an NMR

study revealed that, despite being intrinsically disordered in solution, Pγ also exhibits transient secondary structure.[9] Generally, IDPs undergo a disorder-to-order transition upon interaction with their functional partners, with C_8E_4 having the most significant effect on PDE6, not only stabilizing Pγ but also interacting with the isoprenyl groups of PDE6 and either displacing the PrBP/δ–GST protein from the complex or interfering with the binding to PrBP/δ. Micelles of C_8E_4 may restrict the movement of Pγ and help to keep it in place. The stabilizing effect of detergents was more detergent-specific than concentration-dependent. The presence of polyoxylethylene micelles could be useful in masking the isoprenylated C-terminal regions of PDE6 and reducing PDE6 heterogeneity.

However, we did not observe a direct interaction between detergents and PDE6. On the basis of SEC analysis, elution profiles of PDE6 were the same in the presence or absence of detergents. There were no obvious size changes conferred by the presence of detergents. So how do detergents stabilize PDE6? Pγ is rich in Pro residues and positively charged amino acid residues in its central region. This property may allow the peptide to interact more favorably with certain types of detergents such as C_8E_4. It is likely that detergent micelles can effectively surround hydrophobic patches on Pγ, restricting its movements and stabilizing its blockage of sites of entry into PDE6 catalytic domains.

Hydrophobic interaction chromatography succeeded in quantitatively separating glutamic acid-rich protein (GARP2) from the PDE6 holoenzyme.[48] Moreover, PrBP/δ also releases PDE6 from ROS without solubilization of GARP2.[48] In a manner consistent with this report, we have not observed GARP2 in our preparations when PDE6 was released from rod membranes with the PrBP/δ–GST protein. On the basis of these observations, we speculate that C_8E_4 likely would dissociate GARP2 from PDE6 when added to ROS membranes, but this detergent will also solubilize a fraction of rhodopsin, causing problems with further investigation of this enzyme in a biochemically acceptable form. The effect of this detergent on transducin will require additional study if the goal is to isolate the PDE6–transducin complex. Another unexplored area of investigation is determining if blocking the active site with filmy attached Pγ-C_8E_4 will prevent or allow binding of nucleoside inhibitors.

In summary, we have demonstrated that certain types of detergents suppress the basal enzymatic activity of PDE6, presumably by stabilizing its structure. These detergents did not decrease the catalytic ability of activated PDE6. Moreover, the same detergents interacted with the C-termini of PDE6 and dissociated the PrBP/δ–GST protein from the ternary complex. An extensive body of literature demonstrates the effectiveness of including detergents in crystallization trials to prevent non-specific aggregation due to hydrophobic interactions. This is further supported by our EM studies that illustrate a strategy for screening detergents quickly that allow PDE6 to retain its homogeneity. Detergents may play a critical role in the eventual structural characterization of the PDE6 complex.

■ ASSOCIATED CONTENT

Ⓢ Supporting Information

Descriptions of PDE6 activity measurements using the pH-sensitive fluorescent dye SNARF-1 and HPLC and size exclusion chromatography of the PDE6 conformation in the presence of C_8E_4. This material is available free of charge via the Internet at http://pubs.acs.org.

■ AUTHOR INFORMATION

Corresponding Author

*Phone: (216) 368-4631. Fax: (216) 368-1300. E-mail: kxp65@case.edu.

Funding

This research was supported, in whole or in part, by National Institutes of Health Grants EY009339 and P30 EY11373. K.P. is the John H. Hord Professor of Pharmacology.

■ ACKNOWLEDGMENTS

We thank Dr. Leslie T. Webster, Jr., and the Palczewski laboratory for critical comments on the manuscript. We thank Susan Farr and Dr. Beata Jastrzebska for helping with PDE6 preparation, Professor John Mieyal for comments on PDE6 activity assays and using the instrument, and Heather Holdaway for technical assistance with electronic microscopy.

■ ABBREVIATIONS

Anapoe-35, polyethylene glycol monododecyl ether 23; Bis-Tris, bis(2-hydroxyethyl)-aminotris(hydroxymethyl)methane; $C_{12}E_8$, octyloxyethylene 8-dodecyl ether; C_8E_4, tetraethylene glycol monooctyl ether; cGMP, cyclic guanosine 3′,5′-monophosphate; CHAPS, 3-[(3-cholamidopropyl)dimethylammonio]-1-propanesulfonate; CMC, critical micelle concentration; C_nE_m, C_n = $CH_3(CH_2)_{n-1}$ alkyl chain, E_m = $(OCH_2CH_2)_mOH$ oligoethylene glycol; CYGLU-3, 3-cyclohexyl-1-propyl β-D-glucoside; Cymal-6, 6-cyclohexyl-1-hexyl β-D-maltoside; DDM, *n*-dodecyl α-D-maltopyranoside; GST, glutathione *S*-transferase; IDP, intrinsically disordered protein; MEGA-8, octanoyl *N*-methylglucanide; PG, PDE6–PrBP/δ–GST; PMAL-C8, poly(maleic anhydride-alt-1-decene) substituted with 3-(dimethylamino)propylamine; PrBP/δ, isoprenyl-binding protein δ; Pγ, inhibitory γ subunit of PDE6; ROS, rod outer segment(s); SEC, size exclusion chromatography; $T_{1/2}$, half-life.

■ REFERENCES

(1) Polans, A., Baehr, W., and Palczewski, K. (1996) Turned on by Ca^{2+}! The physiology and pathology of Ca^{2+}-binding proteins in the retina. *Trends Neurosci. 19*, 547–554.

(2) Conti, M., and Beavo, J. (2007) Biochemistry and physiology of cyclic nucleotide phosphodiesterases: Essential components in cyclic nucleotide signaling. *Annu. Rev. Biochem. 76*, 481–511.

(3) Artemyev, N. O., Surendran, R., Lee, J. C., and Hamm, H. E. (1996) Subunit structure of rod cGMP-phosphodiesterase. *J. Biol. Chem. 271*, 25382–25388.

(4) Baehr, W., Devlin, M. J., and Applebury, M. L. (1979) Isolation and characterization of cGMP phosphodiesterase from bovine rod outer segments. *J. Biol. Chem. 254*, 11669–11677.

(5) Deterre, P., Bigay, J., Forquet, F., Robert, M., and Chabre, M. (1988) cGMP phosphodiesterase of retinal rods is regulated by two inhibitory subunits. *Proc. Natl. Acad. Sci. U.S.A. 85*, 2424–2428.

(6) Artemyev, N. O., and Hamm, H. E. (1992) Two-site high-affinity interaction between inhibitory and catalytic subunits of rod cyclic GMP phosphodiesterase. *Biochem. J. 283* (Part 1), 273–279.

(7) Artemyev, N. O., Rarick, H. M., Mills, J. S., Skiba, N. P., and Hamm, H. E. (1992) Sites of interaction between rod G-protein α-subunit and cGMP-phosphodiesterase γ-subunit. Implications for the phosphodiesterase activation mechanism. *J. Biol. Chem. 267*, 25067–25072.

(8) Hurley, J. B., and Stryer, L. (1982) Purification and characterization of the γ regulatory subunit of the cyclic GMP phosphodiesterase from retinal rod outer segments. *J. Biol. Chem. 257*, 11094–11099.

(9) Song, J., Guo, L. W., Muradov, H., Artemyev, N. O., Ruoho, A. E., and Markley, J. L. (2008) Intrinsically disordered γ-subunit of

cGMP phosphodiesterase encodes functionally relevant transient secondary and tertiary structure. *Proc. Natl. Acad. Sci. U.S.A. 105*, 1505−1510.

(10) Anant, J. S., Ong, O. C., Xie, H. Y., Clarke, S., O'Brien, P. J., and Fung, B. K. (1992) In vivo differential prenylation of retinal cyclic GMP phosphodiesterase catalytic subunits. *J. Biol. Chem. 267*, 687−690.

(11) Qin, N., and Baehr, W. (1994) Expression and mutagenesis of mouse rod photoreceptor cGMP phosphodiesterase. *J. Biol. Chem. 269*, 3265−3271.

(12) Christiansen, J. R., Kolandaivelu, S., Bergo, M. O., and Ramamurthy, V. (2011) RAS-converting enzyme 1-mediated endoproteolysis is required for trafficking of rod phosphodiesterase 6 to photoreceptor outer segments. *Proc. Natl. Acad. Sci. U.S.A. 108*, 8862−8866.

(13) Cook, T. A., Ghomashchi, F., Gelb, M. H., Florio, S. K., and Beavo, J. A. (2000) Binding of the δ subunit to rod phosphodiesterase catalytic subunits requires methylated, prenylated C-termini of the catalytic subunits. *Biochemistry 39*, 13516−13523.

(14) Goc, A., Chami, M., Lodowski, D. T., Bosshart, P., Moiseenkova-Bell, V., Baehr, W., Engel, A., and Palczewski, K. (2010) Structural Characterization of the Rod cGMP Phosphodiesterase 6. *J. Mol. Biol. 401*, 363−373.

(15) Pandit, J., Forman, M. D., Fennell, K. F., Dillman, K. S., and Menniti, F. S. (2009) Mechanism for the allosteric regulation of phosphodiesterase 2A deduced from the X-ray structure of a near full-length construct. *Proc. Natl. Acad. Sci. U.S.A. 106*, 18225−18230.

(16) Xu, R. X., Hassell, A. M., Vanderwall, D., Lambert, M. H., Holmes, W. D., Luther, M. A., Rocque, W. J., Milburn, M. V., Zhao, Y., Ke, H., and Nolte, R. T. (2000) Atomic structure of PDE4: Insights into phosphodiesterase mechanism and specificity. *Science 288*, 1822−1825.

(17) Sung, B. J., Hwang, K. Y., Jeon, Y. H., Lee, J. I., Heo, Y. S., Kim, J. H., Moon, J., Yoon, J. M., Hyun, Y. L., Kim, E., Eum, S. J., Park, S. Y., Lee, J. O., Lee, T. G., Ro, S., and Cho, J. M. (2003) Structure of the catalytic domain of human phosphodiesterase 5 with bound drug molecules. *Nature 425*, 98−102.

(18) Barren, B., Gakhar, L., Muradov, H., Boyd, K. K., Ramaswamy, S., and Artemyev, N. O. (2009) Structural basis of phosphodiesterase 6 inhibition by the C-terminal region of the γ-subunit. *EMBO J. 28*, 3613−3622.

(19) Grizot, S., Faure, J., Fieschi, F., Vignais, P. V., Dagher, M. C., and Pebay-Peyroula, E. (2001) Crystal structure of the Rac1-RhoGDI complex involved in NADPH oxidase activation. *Biochemistry 40*, 10007−10013.

(20) Zhang, H., Constantine, R., Vorobiev, S., Chen, Y., Seetharaman, J., Huang, Y. J., Xiao, R., Montelione, G. T., Gerstner, C. D., Davis, M. W., Inana, G., Whitby, F. G., Jorgensen, E. M., Hill, C. P., Tong, L., and Baehr, W. (2011) UNC119 is required for G protein trafficking in sensory neurons. *Nat. Neurosci. 14*, 874−880.

(21) Kajimura, N., Yamazaki, M., Morikawa, K., Yamazaki, A., and Mayanagi, K. (2002) Three-dimensional structure of non-activated cGMP phosphodiesterase 6 and comparison of its image with those of activated forms. *J. Struct. Biol. 139*, 27−38.

(22) Granovsky, A. E., Natochin, M., McEntaffer, R. L., Haik, T. L., Francis, S. H., Corbin, J. D., and Artemyev, N. O. (1998) Probing domain functions of chimeric PDE6α'/PDE5 cGMP-phosphodiesterase. *J. Biol. Chem. 273*, 24485−24490.

(23) Liu, X., Bulgakov, O. V., Wen, X. H., Woodruff, M. L., Pawlyk, B., Yang, J., Fain, G. L., Sandberg, M. A., Makino, C. L., and Li, T. (2004) AIPL1, the protein that is defective in Leber congenital amaurosis, is essential for the biosynthesis of retinal rod cGMP phosphodiesterase. *Proc. Natl. Acad. Sci. U.S.A. 101*, 13903−13908.

(24) Kolandaivelu, S., Huang, J., Hurley, J. B., and Ramamurthy, V. (2009) AIPL1, a protein associated with childhood blindness, interacts with α-subunit of rod phosphodiesterase (PDE6) and is essential for its proper assembly. *J. Biol. Chem. 284*, 30853−30861.

(25) Okada, T., Le Trong, I., Fox, B. A., Behnke, C. A., Stenkamp, R. E., and Palczewski, K. (2000) X-ray diffraction analysis of three-dimensional crystals of bovine rhodopsin obtained from mixed micelles. *J. Struct. Biol. 130*, 73−80.

(26) Wang, G. (2008) NMR of membrane-associated peptides and proteins. *Curr. Protein Pept. Sci. 9*, 50−69.

(27) Dobrovetsky, E., Menendez, J., Edwards, A. M., and Koth, C. M. (2007) A robust purification strategy to accelerate membrane proteomics. *Methods 41*, 381−387.

(28) Caffrey, M. (2003) Membrane protein crystallization. *J. Struct. Biol. 142*, 108−132.

(29) Cudney, R., Patel, S., Weisgraber, K., Newhouse, Y., and McPherson, A. (1994) Screening and optimization strategies for macromolecular crystal growth. *Acta Crystallogr. D50*, 414−423.

(30) Papermaster, D. S. (1982) Preparation of retinal rod outer segments. *Methods Enzymol. 81*, 48−52.

(31) Bradford, M. M. (1976) A rapid and sensitive method for the quantitation of microgram quantities of protein utilizing the principle of protein-dye binding. *Anal. Biochem. 72*, 248−254.

(32) Brown, R. L. (1992) Functional regions of the inhibitory subunit of retinal rod cGMP phosphodiesterase identified by site-specific mutagenesis and fluorescence spectroscopy. *Biochemistry 31*, 5918−5925.

(33) Goc, A., Angel, T. E., Jastrzebska, B., Wang, B., Wintrode, P. L., and Palczewski, K. (2008) Different properties of the native and reconstituted heterotrimeric G protein transducin. *Biochemistry 47*, 12409−12419.

(34) Pentia, D. C., Hosier, S., Collupy, R. A., Valeriani, B. A., and Cote, R. H. (2005) Purification of PDE6 isozymes from mammalian retina. *Methods Mol. Biol. 307*, 125−140.

(35) Catty, P., Pfister, C., Bruckert, F., and Deterre, P. (1992) The cGMP phosphodiesterase-transducin complex of retinal rods. Membrane binding and subunits interactions. *J. Biol. Chem. 267*, 19489−19493.

(36) Gillespie, P. G., and Beavo, J. A. (1989) Inhibition and stimulation of photoreceptor phosphodiesterases by dipyridamole and M&B 22,948. *Mol. Pharmacol. 36*, 773−781.

(37) Gillespie, P. G., and Beavo, J. A. (1989) cGMP is tightly bound to bovine retinal rod phosphodiesterase. *Proc. Natl. Acad. Sci. U.S.A. 86*, 4311−4315.

(38) Gillespie, P. G., Prusti, R. K., Apel, E. D., and Beavo, J. A. (1989) A soluble form of bovine rod photoreceptor phosphodiesterase has a novel 15-kDa subunit. *J. Biol. Chem. 264*, 12187−12193.

(39) Mou, H., Grazio, H. J. III, Cook, T. A., Beavo, J. A., and Cote, R. H. (1999) cGMP binding to noncatalytic sites on mammalian rod photoreceptor phosphodiesterase is regulated by binding of its γ and δ subunits. *J. Biol. Chem. 274*, 18813−18820.

(40) Muradov, H., Boyd, K. K., and Artemyev, N. O. (2010) Rod phosphodiesterase-6 PDE6A and PDE6B subunits are enzymatically equivalent. *J. Biol. Chem. 285*, 39828−39834.

(41) Malinski, J. A., and Wensel, T. G. (1992) Membrane stimulation of cGMP phosphodiesterase activation by transducin: Comparison of phospholipid bilayers to rod outer segment membranes. *Biochemistry 31*, 9502−9512.

(42) Wensel, T. G., and Stryer, L. (1986) Reciprocal control of retinal rod cyclic GMP phosphodiesterase by its γ subunit and transducin. *Proteins 1*, 90−99.

(43) Skiba, N. P., Artemyev, N. O., and Hamm, H. E. (1995) The carboxyl terminus of the γ-subunit of rod cGMP phosphodiesterase contains distinct sites of interaction with the enzyme catalytic subunits and the α-subunit of transducin. *J. Biol. Chem. 270*, 13210−13215.

(44) Takemoto, D. J., Hurt, D., Oppert, B., and Cunnick, J. (1992) Domain mapping of the retinal cyclic GMP phosphodiesterase γ-subunit. Function of the domains encoded by the three exons of the γ-subunit gene. *Biochem. J. 281* (Part 3), 637−643.

(45) Muradov, K. G., Granovsky, A. E., Schey, K. L., and Artemyev, N. O. (2002) Direct interaction of the inhibitory γ-subunit of rod cGMP phosphodiesterase (PDE6) with the PDE6 GAFa domains. *Biochemistry 41*, 3884−3890.

(46) Guo, L. W., Assadi-Porter, F. M., Grant, J. E., Wu, H., Markley, J. L., and Ruoho, A. E. (2007) One-step purification of bacterially

expressed recombinant transducin α-subunit and isotopically labeled PDE6 γ-subunit for NMR analysis. *Protein Expression Purif. 51*, 187–197.

(47) Uversky, V. N., Permyakov, S. E., Zagranichny, V. E., Rodionov, I. L., Fink, A. L., Cherskaya, A. M., Wasserman, L. A., and Permyakov, E. A. (2002) Effect of zinc and temperature on the conformation of the γ subunit of retinal phosphodiesterase: A natively unfolded protein. *J. Proteome Res. 1*, 149–159.

(48) Pentia, D. C., Hosier, S., and Cote, R. H. (2006) The glutamic acid-rich protein-2 (GARP2) is a high affinity rod photoreceptor phosphodiesterase (PDE6)-binding protein that modulates its catalytic properties. *J. Biol. Chem. 281*, 5500–5505.